

Constraints on global CPV parameters including the new LHCb $D^0 \rightarrow K\pi$ measurements

R. Andreassen¹, A. Davis¹, M.D. Sokoloff¹
¹*University of Cincinnati*

Abstract

The new $D^0 \rightarrow K\pi$ result from LHCb provides a credibly powerful constraint on mixing parameters. This note describes a fit in the style of HFAG to combine our result with previous measurements.

Contents

1	Introduction	1
2	Chi-square calculation	1
3	Fit variants	2
4	Measurements Used	4
5	Results	4
5.1	HFAG 2013 Validation	4
5.2	No CP Violation Allowed	5
5.3	No Direct CP Violation Allowed	5
5.4	All CP Violation Allowed	8
6	Conclusion	8
	References	8

1 Introduction

To fully understand the global impact of the updated WS $D^0 \rightarrow K\pi$ analysis, a combination of global results of the neutral D system is necessary. We present an HFAG-like fit for the underlying parameters $|q/p|$, ϕ , x and y , combining the updated 2011+2012 LHCb $D^0 \rightarrow K\pi$ results with older results from HFAG. We find that the LHCb measurement, with its small difference between plus-superscript and minus-superscript values, is a powerful constraint on the value of $|q/p|$. In the case of no direct CP violation, the error drops from the current HFAG average of about 7% down to a mere 1.3%. It is less powerful in constraining x and y .

For this study we do three kinds of fits: “Type 1”, where we assume no CP violation, “Type 2” where only indirect CP violation is allowed, and “Type 3” where all the CP-violating parameters are allowed to float independently. In each case, we study how the fit results, and especially the χ^2 , change in response to considering subsets of the possible inputs; we find that some measurements are very heavy contributors to χ^2 , but removing them does not much change the fit results.

2 Chi-square calculation

The purpose of our fit is to combine the errors on several different measurements of the same parameters, where each measurement may have a different relation to the underlying true mixing parameters (eg measuring (x'^2, y') in place of (x, y)), and where the numbers

in each measurement may be strongly correlated. To do so we construct an overall χ^2 for all the results:

$$\chi^2 = \vec{\epsilon}^T \sigma^{-1} \vec{\epsilon} \quad (1)$$

where the elements of $\vec{\epsilon}$ are given by $\epsilon_i = m_i - p_i$. Here \vec{m} is the list of measured values from experiments, and \vec{p} is a set of “proposed” values for the mixing parameters; we use MINUIT to vary \vec{p} so as to minimise χ^2 . Finally, σ is an $N \times N$ matrix where N is the number of measurements, with $\sigma_{ij} = e_i c_{ij} e_j$. Here e_i is the reported error on measurement i , and c_{ij} is the correlation coefficient between measurements i and j .

Notice that, if the measurements are uncorrelated, then σ reduces to a diagonal matrix where the elements are the squares of the measurement errors. In this case χ^2 is simply the sum $\sum_i \epsilon_i^2 / e_i^2$, that is, each element is the difference between a measurement and the corresponding prediction, divided by the error on the measurement, squared. In other words, if there are no correlations we recover the usual chi-square goodness-of-fit metric.

3 Fit variants

In full generality, we wish to fit for no less than seven underlying related mixing parameters:

- x and y , the normalised mass and width differences
- R_D^+ and R_D^- , the ratios of rates
- δ , the strong phase difference in the $D^0 \rightarrow K\pi$ channel
- $|q/p|$ and ϕ , the magnitude and phase of the indirect CP violation.

The observed inputs, however, are not all direct measurements of these quantities. From $D^0 \rightarrow K_S \pi \pi$ we get direct measurements of x , y , $|q/p|$ and ϕ ; $D^0 \rightarrow K\pi$ results also yield R_D^\pm directly, although sometimes quoted as $R_D = \frac{1}{2}(R_D^+ + R_D^-)$ and $A_D = \frac{R_D^+ - R_D^-}{R_D^+ + R_D^-}$. However, we also measure the derived parameters $x'^{2(\pm)}$, $y'^{(\pm)}$, y_{CP} , and A_Γ , defined as:

$$x' = x \cos \delta + y \sin \delta \quad (2)$$

$$y' = y \cos \delta - x \sin \delta \quad (3)$$

$$x'^{\pm} = \left(\frac{1 \pm A_M}{1 \mp A_M} \right)^{1/4} (x' \cos \phi \pm y' \sin \phi) \quad (4)$$

$$y'^{\pm} = \left(\frac{1 \pm A_M}{1 \mp A_M} \right)^{1/4} (y' \cos \phi \mp x' \sin \phi) \quad (5)$$

$$2y_{CP} = (|q/p| + |p/q|) y \cos \phi - (|q/p| - |p/q|) x \sin \phi \quad (6)$$

$$2A_\Gamma = (|q/p| - |p/q|) y \cos \phi - (|q/p| + |p/q|) x \sin \phi \quad (7)$$

$$(8)$$

where the helper quantity A_M is given by

$$A_M = \frac{|q/p|^2 - |p/q|^2}{|q/p|^2 + |p/q|^2}. \quad (9)$$

To calculate $\vec{\epsilon}$, then, we take in a vector of proposed mixing parameters from MINUIT, calculate the resulting observable parameters from the equations above, and subtract the actually observed numbers.

In addition to the fully-general fit allowing all these variables to float, there are some variants imposing different no-CPV constraints:

- No CP violation. In this fit we set $|q/p| = 1$, $\phi = 0$, and $R_D^+ = R_D^-$, and fit only for x , y , δ , and R_D .
- No direct CP violation. With no direct CP violation, $R_D^+ = R_D^-$; in addition, the four parameters x , y , ϕ and $|q/p|$ are related (in the limit that CPV is small) by the constraint

$$|q/p| = \sqrt{\frac{x - y \tan \phi}{x + y \tan \phi}} \quad (10)$$

$$\phi = \tan^{-1} \left(\frac{1 - |q/p|^2 x}{1 + |q/p|^2 y} \right) \quad (11)$$

Thus, to extract errors on both variables, we have two variants on this fit:

2a Here we allow $|q/p|$ to float and calculate ϕ from the constraint.

2b We allow ϕ to float and calculate $|q/p|$ from the constraint.

- All CPV allowed. As A_D is quite small, the contribution of a new physics phase to ϕ is far below our current sensitivity; consequently the constraint above is a reasonable approximation. We therefore run three variants of the all-CPV-allowed scenario:

3a All parameters float, no constraint.

3b ϕ is calculated from $|q/p|$ as above, rather than allowed to float. R_D^+ and R_D^- are both free, as before.

3c As in 3b, but with $|q/p|$ calculated from the constraint and ϕ allowed to float.

In addition, we do a fit not allowing direct CP violation, in which the free parameters are the underlying¹ x_{12} , y_{12} , and ϕ_{12} . These parameters are related (in the limit of no

¹See Kagan and Sokoloff, Phys.Rev.D80:076008 (2009), <http://arxiv.org/abs/0907.3917>.

65 direct CP violation) to $|q/p|$, x , y and ϕ (no subscripts!) as follows:

$$x = \frac{1}{\sqrt{2}} \text{sign}(\cos \phi_{12}) \sqrt{x_{12}^2 - y_{12}^2 + |x_{12}^2 + y_{12}^2| - 4x_{12}^2 y_{12}^2 \sin^2(\phi_{12})} \quad (12)$$

$$y = \frac{1}{\sqrt{2}} \left(y_{12}^2 - x_{12}^2 + \sqrt{(x_{12}^2 + y_{12}^2)^2 - 4x_{12}^2 y_{12}^2 \sin^2(\phi_{12})} \right)^{1/2} \quad (13)$$

$$|q/p| = \left(\frac{x_{12}^2 + y_{12}^2 + 2x_{12}y_{12}\sin(\phi_{12})}{x_{12}^2 + y_{12}^2 - 2x_{12}y_{12}\sin(\phi_{12})} \right)^{1/4} \quad (14)$$

$$\phi = -\frac{1}{2} \frac{\sin(2\phi_{12})}{\cos(2\phi_{12}) + \frac{y_{12}^2}{x_{12}^2}}. \quad (15)$$

66 Our approach in this fit is to allow MINUIT to believe that the parameters x_{12} , y_{12} , and
 67 ϕ_{12} are free, but calculate the non-underlying² parameters x , y , ϕ , and $|q/p|$, and use these
 68 values in the calculation of χ^2 , as outlined for the other fits.

69 4 Measurements Used

70 As input for the fit method, all results from many different experiments have been
 71 compiled. Table 1 lists all the possible measurements pertaining to fits excluding CP
 72 Violation. Table 2 corresponds to measurements allowing only direct CP violation, and
 73 Table 3 lists all measurements pertaining to both direct and indirect CP violation allowed.
 74 As a starting point, all measurements are used in the fit. However, the BaBar $K\pi$ results
 75 add a large χ^2 value to the fit. By systematically removing measurements from the total
 76 fit, we study the effect on the total χ^2 of the fit.

77

78 Additionally, as the LHCb A_Γ results are not yet published, we choose to do sets of
 79 fits both including and excluding this result.

80 5 Results

81 The results are split into subsections depending on the type of CP Violation allowed.
 82 Additionally, results are presented using a variety of different combinations of the available
 83 data. Figure 1 shows all variations for the no CPV allowed fits. Figure 4 shows the results
 84 for a subset of variations on All CPV allowed fits.

85 5.1 HFAG 2013 Validation

86 In order to insure that our fit is robust, we attempt to reproduce the April 2013 results
 87 of the HFAG collaboration [1]. The results of this fit are listed in Table 4. Results are

²Overlying?

Result	Value	Correlation Coefficients		
HFAG y_{CP}	$(8.66 \pm 1.55) \times 10^{-3}$			
LHCb R_D	$(3.568 \pm 0.058 \pm 0.033) \times 10^{-3}$	1	0.869	-0.953
LHCb $x'^2(K\pi)$	$(5.5 \pm 4.2 \pm 2.6) \times 10^{-5}$		1	-0.967
LHCb $y'(K\pi)$	$(4.81 \pm 0.85 \pm 0.53) \times 10^{-3}$			1
HFAG $x(K_S^0\pi\pi)$	$(4.19 \pm 2.11 \pm 0) \times 10^{-3}$			
HFAG $y(K_S^0\pi\pi)$	$(4.56 \pm 1.86) \times 10^{-3}$			
CLEO $\cos(\delta)(K\pi)$	$0.81 \pm 0.2 \pm 0.06$			
CLEO $\sin(\delta)(K\pi)$	$-0.01 \pm 0.41 \pm 0.04$			
CDF R_D	$(3.04 \pm 0.55) \times 10^{-3}$	1	0.923	-0.87
CDF $x'^2(K\pi)$	$(-1.2 \pm 3.5 \pm 0) \times 10^{-4}$		1	-0.984
CDF $y'(K\pi)$	$(8.5 \pm 7.6) \times 10^{-3}$			1
Belle R_D	$(3.64 \pm 0.17) \times 10^{-3}$	1	0.655	-0.834
Belle $x'^2(K\pi)$	$(1.8 \pm 2.2) \times 10^{-4}$		1	-0.909
Belle $y'(K\pi)$	$(0.6 \pm 4.0) \times 10^{-3}$			1
BaBar R_D	$(3.03 \pm 0.16 \pm 0.1) \times 10^{-3}$	1	0.77	-0.87
BaBar $x'^2(K\pi)$	$(-2.2 \pm 3.0 \pm 2.1) \times 10^{-4}$		1	-0.94
BaBar $y'(K\pi)$	$(9.7 \pm 4.4 \pm 3.1) \times 10^{-3}$			1

Table 1: No CPV allowed inputs. Correlation coefficients follow the listing in the first column.

statistically equivalent and many errors are reproduced. The main differences stem from the fact that not all of the results listed from the HFAG website [1] are used in our fit. However, the fact that many of the errors are reproduced ensures that the dominant contributions to the fit are accurate.

5.2 No CP Violation Allowed

Table 5 lists the results from the No CP Violation allowed global fit. As $A_\Gamma = 0$ in the case of No CPV, the data is not included in this fit. Additionally, we take subsets of the data which do not include results from Belle, BaBar and CDF in order to explore the change in χ^2/ndf of the global fit.

5.3 No Direct CP Violation Allowed

As opposed to the No CP violation case, allowing CP violation excepting direct CP Violation allows the inclusion of additional global results. For instance, the preliminary result for A_Γ from KK and $\pi\pi$ as reported by LHCb Table 6 lists the results of the global fit without direct CP violation, but excluding the preliminary LHCb A_Γ results. The complementary results including the LHCb A_Γ results are listed in Table 7. The inclusion

Result	Value	Correlation Coefficients				
HFAG y_{CP}	$(8.66 \pm 1.55) \times 10^{-3}$					
HFAG A_Γ	$(-0.22 \pm 1.61) \times 10^{-3}$					
LHCb $A_\Gamma(KK)$	$(-0.35 \pm 0.62 \pm 0.12) \times 10^{-3}$					
LHCb $A_\Gamma(\pi\pi)$	$(0.33 \pm 1.06 \pm 0.14) \times 10^{-3}$					
LHCb R_D	$(3.568 \pm 0.058 \pm 0.033) \times 10^{-3}$	1	-0.902	0.773	-0.902	0.777
LHCb $y'^+(K\pi)$	$(4.46 \pm 0.89 \pm 0.57) \times 10^{-3}$		1	-0.948	0.795	-0.686
LHCb $x'^{2+}(K\pi)$	$(7.7 \pm 4.6 \pm 2.9) \times 10^{-5}$			1	-0.684	0.591
LHCb $y'^-(K\pi)$	$(5.17 \pm 0.89 \pm 0.58) \times 10^{-3}$				1	-0.950
LHCb $x'^{2-}(K\pi)$	$(3.2 \pm 4.7 \pm 3.0) \times 10^{-5}$					1
Belle $x(K_S^0\pi\pi)$	$(8.11 \pm 3.34) \times 10^{-3}$					
Belle $y(K_S^0\pi\pi)$	$(3.09 \pm 2.81) \times 10^{-3}$					
Belle $ q/p $	$0.95 \pm 0.22 \pm 0.1$					
Belle ϕ	$-0.035 \pm 0.19 \pm 0.09$					
CLEO R_D	$(5.33 \pm 1.07 \pm 0.45) \times 10^{-3}$	1	0.000	0.000	-0.420	0.010
CLEO $x'^2(K\pi)$	$(0.6 \pm 2.3 \pm 1.1) \times 10^{-3}$		1	-0.730	0.390	0.020
CLEO $y'(K\pi)$	$(4.2 \pm 2.0 \pm 1.0) \times 10^{-2}$			1	-0.530	-0.030
CLEO $\cos(\delta)(K\pi)$	$0.81 \pm 0.2 \pm 0.06$				1	0.040
CLEO $\sin(\delta)(K\pi)$	$-0.01 \pm 0.41 \pm 0.04$					1
CDF R_D	$(3.04 \pm 0.55) \times 10^{-3}$		1	0.923	-0.971	
CDF $x'^2(K\pi)$	$(-1.2 \pm 3.5) \times 10^{-4}$			1	-0.984	
CDF $y'(K\pi)$	$(8.5 \pm 7.6 \pm 0) \times 10^{-3}$				1	
Belle R_D	$(3.64 \pm 0.18) \times 10^{-3}$	1	0.655	-0.834	0.655	-0.834
Belle $x'^{2-}(K\pi)$	$(0.6 \pm 3.4) \times 10^{-4}$		1	-0.909		
Belle $y'^-(K\pi)$	$(2.0 \pm 5.4) \times 10^{-3}$			1		
Belle $x'^{2+}(K\pi)$	$(3.2 \pm 3.7) \times 10^{-4}$				1	-0.909
Belle $y'^+(K\pi)$	$(-1.2 \pm 5.8) \times 10^{-3}$					1
BaBar R_D	$(3.03 \pm 0.189) \times 10^{-3}$	1	0.77	-0.87	0.77	-0.87
BaBar $x'^{2-}(K\pi)$	$(-2.0 \pm 5.0) \times 10^{-4}$		1	-0.94		
BaBar $y'^-(K\pi)$	$(9.6 \pm 7.5) \times 10^{-3}$			1		
BaBar $x'^{2+}(K\pi)$	$(-2.4 \pm 5.2) \times 10^{-4}$				1	-0.909
BaBar $y'^+(K\pi)$	$(9.8 \pm 7.8) \times 10^{-3}$					1
BaBar $x(K_S^0\pi\pi)$	$(1.6 \pm 2.3 \pm 1.2) \times 10^{-3}$		1	0.0615		
BaBar $y(K_S^0\pi\pi)$	$(5.7 \pm 2.0 \pm 1.3) \times 10^{-3}$			1		

Table 2: No Direct CPV allowed inputs. Correlation coefficients follow the order listed in the first column.

103 of this result does not change the central values or errors substantially. Additionally, in all
104 cases, the error on $|q/p|$ is of order 1.3%.
105 As described in Section 3, it is possible to invert the relationship between $|q/p|$ and ϕ

Result	Value	Correlation Coefficients					
HFAG y_{CP}	$(8.66 \pm 1.55) \times 10^{-3}$						
HFAG A_Γ	$(-0.22 \pm 1.61) \times 10^{-3}$						
LHCb $A_\Gamma(K\bar{K})$	$(-0.35 \pm 0.62 \pm 0.12) \times 10^{-3}$						
LHCb $A_\Gamma(\pi\pi)$	$(0.33 \pm 1.06 \pm 0.14) \times 10^{-3}$						
LHCb R_D^+	$(3.523 \pm 0.081 \pm 0.047) \times 10^{-3}$	1	-0.947	0.866	-0.006	-0.007	0.006
LHCb $y'^+(K\pi)$	$(5.1 \pm 1.2 \pm 0.7) \times 10^{-3}$		1	-0.968	-0.007	0.007	-0.007
LHCb $x'^{2+}(K\pi)$	$(4.9 \pm 6.0 \pm 3.6) \times 10^{-5}$			1	0.006	-0.007	0.008
LHCb R_D^-	$(3.613 \pm 0.082 \pm 0.047) \times 10^{-3}$				1	-0.946	0.862
LHCb $y'^-(K\pi)$	$(4.5 \pm 1.2 \pm 0.7) \times 10^{-3}$					1	-0.966
LHCb $x'^{2-}(K\pi)$	$(6.0 \pm 5.8 \pm 3.6) \times 10^{-5}$						1
Belle $x(K_S^0\pi\pi)$	$(8.1 \pm 3.0 \pm 1.5) \times 10^{-3}$		1	-0.007	-0.510	0.216	
Belle $y(K_S^0\pi\pi)$	$(3.7 \pm 2.5 \pm 1.2) \times 10^{-3}$			1	-0.038	-0.280	
Belle $ q/p $	$0.86 \pm 0.3 \pm 0.1$				1	-0.266	
Belle ϕ	$-0.244 \pm 0.31 \pm 0.09$					1	
CLEO R_D	$(5.33 \pm 1.07 \pm 0.45) \times 10^{-3}$		1	0.000	0.000	-0.420	0.010
CLEO $x^2(K\pi)$	$(0.6 \pm 2.3 \pm 1.1) \times 10^{-3}$			1	-0.730	0.390	0.020
CLEO $y(K\pi)$	$(4.2 \pm 2.0 \pm 1.0) \times 10^{-2}$				1	-0.530	-0.030
CLEO $\cos(\delta)(K\pi)$	$0.81 \pm 0.2 \pm 0.06$					1	0.040
CLEO $\sin(\delta)(K\pi)$	$-0.01 \pm 0.41 \pm 0.04$						1
CDF R_D	$(3.04 \pm 0.55) \times 10^{-3}$			1	0.923	-0.971	
CDF $x'^2(K\pi)$	$(-1.2 \pm 3.5) \times 10^{-4}$				1	-0.984	
CDF $y'(K\pi)$	$(8.5 \pm 7.6) \times 10^{-3}$					1	
Belle R_D^-	$(3.6 \pm 0.2) \times 10^{-3}$		1	0.655	-0.834		
Belle $x'^{2-}(K\pi)$	$(0.6 \pm 3.4) \times 10^{-4}$			1	-0.909		
Belle $y'^-(K\pi)$	$(2.0 \pm 5.4) \times 10^{-3}$				1		
Belle R_D^+	$(3.68 \pm 0.2) \times 10^{-3}$					1	0.655
Belle $x'^{2+}(K\pi)$	$(3.2 \pm 3.7) \times 10^{-4}$						1
Belle $y'^+(K\pi)$	$(-1.2 \pm 5.8) \times 10^{-3}$						-0.834
BaBar R_D^-	$(3.03 \pm 0.2 \pm 0.1) \times 10^{-3}$		1	0.77	-0.87		
BaBar $x'^{2-}(K\pi)$	$(-2.0 \pm 4.1 \pm 2.9) \times 10^{-4}$			1	-0.94		
BaBar $y'^-(K\pi)$	$(9.6 \pm 6.4 \pm 4.5) \times 10^{-3}$				1		
BaBar R_D^+	$(3.03 \pm 0.2 \pm 0.1) \times 10^{-3}$					1	0.77
BaBar $x'^{2+}(K\pi)$	$(-2.4 \pm 4.3 \pm 3.0) \times 10^{-4}$						1
BaBar $y'^+(K\pi)$	$(9.8 \pm 6.1 \pm 4.3) \times 10^{-3}$						-0.87
BaBar $x(K_S^0\pi\pi)$	$(1.6 \pm 2.3 \pm 1.2) \times 10^{-3}$			1	0.0615		
BaBar $y(K_S^0\pi\pi)$	$(5.7 \pm 2.0 \pm 1.3) \times 10^{-3}$				1		

Table 3: All CPV allowed inputs. Correlation coefficients follow the order listed in the first column.

106 to instead fit for ϕ as the free parameter in the fit. Table 8 lists the results of this fit
107 excluding the preliminary LHCb A_Γ result, and Table 9 lists the results including the
108 preliminary result.

	No CPV	No Direct CPV	All CPV allowed
$x[\%]$	0.318 ± 0.018	0.469 ± 0.186	0.314 ± 0.192
$y[\%]$	0.617 ± 0.075	0.605 ± 0.098	0.675 ± 0.097
$\delta_{K\pi}[\text{deg}]$	4.769 ± 14.458	18.686 ± 10.667	10.421 ± 15.902
$\phi[\text{deg}]$	-	-	-27.897 ± 9.843
$R_D[10^{-3}]$	3.470 ± 0.055	3.720 ± 0.075	
$R_D^-[10^{-3}]$	-	-	3.471 ± 0.093
$R_D^+[10^{-3}]$	-	-	3.418 ± 0.078
$ q/p [\%]$	-	102.947 ± 11.284	82.100 ± 19.693
χ^2/ndf	50.3649/16	22.263/24	59.2804/24

Table 4: Output of the All CP Violation allowed global fit excluding the preliminary LHCb A_Γ measurement. Different Columns list differing subsets of data included in the fit.

	All Results	No BaBar $K\pi$	No Belle, BaBar $K\pi$	No Belle, BaBar, CDF $K\pi$
$x[\%]$	0.378 ± 0.180	0.467 ± 0.183	0.473 ± 0.186	0.474 ± 0.187
$y[\%]$	0.629 ± 0.080	0.649 ± 0.089	0.651 ± 0.090	0.655 ± 0.090
$\delta_{K\pi}[\text{deg}]$	9.334 ± 12.487	14.601 ± 10.694	14.902 ± 10.689	14.550 ± 10.730
$R_D[10^{-3}]$	3.493 ± 0.039	3.542 ± 0.044	3.547 ± 0.047	3.547 ± 0.047
χ^2/ndf	43.8487/16	27.8873/13	24.343/10	13.5119/7

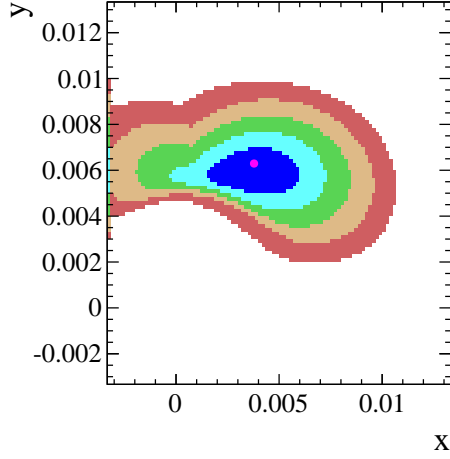
Table 5: Output values of No CPV allowed global fit. Different columns list subsets of allowed data.

5.4 All CP Violation Allowed

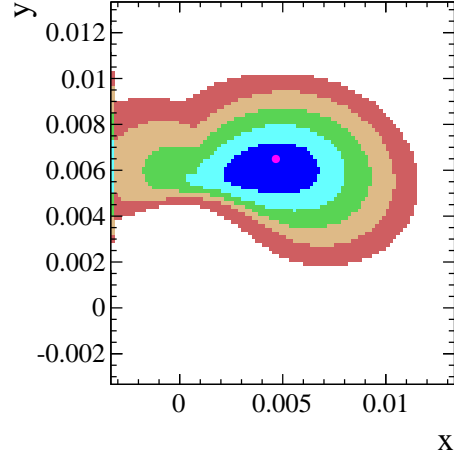
Table 10 lists the results of the global All CP Violation allowed fit. Again, the latter columns list the differing subsets of the data to explore the variation in global χ^2/ndf . The most noticable difference between all fits is the evaluation of x , which varies quite a bit with the inclusion of differing datasets.

6 Conclusion

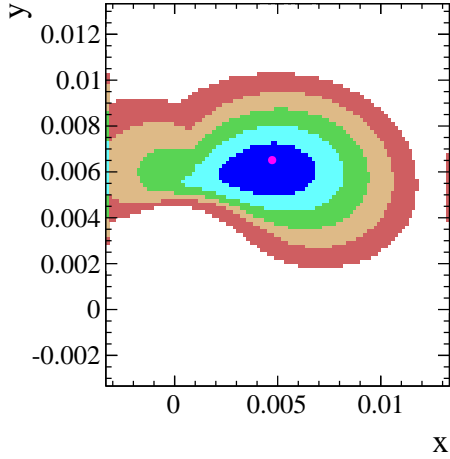
By utilizing a global, HFAG-like fit, we constrain to be $|q/p| = xxxxx \pm yyyyy$ and $\phi = zzzzzzz \pm qqqqqqqqqqqq$, in the case of all CPV allowed. Allowing only direct CPV, $|q/p| = xxxxx \pm yyyyy$ and $\phi = zzzzzzz \pm qqqqqqqqqqqq$. These measurements represent the most precise determination of the CP violating parameters of the natural D meson system



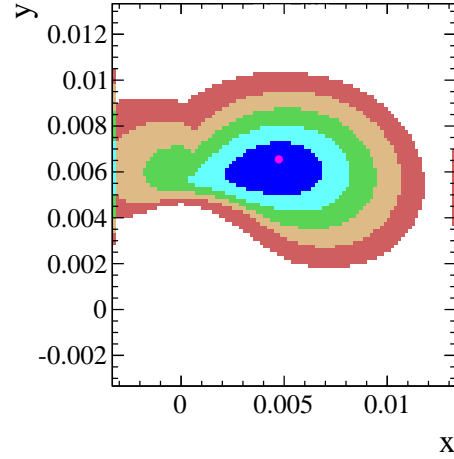
(a) Two dimensional error ellipses for x and y using all measurements listed in Table 5.



(b) Two dimensional error ellipses for x and y using all available measurements except the BaBar $K\pi$ measurements.



(c) Two dimensional error ellipses for x and y from fit excluding Belle and BaBar $K\pi$ results.



(d) Two dimensional error ellipses for x and y from fit excluding Belle, BaBar and CDF measurements.

Figure 1: Two dimensional error ellipses of x and y from fit for No CPV. Exclusion of the Belle and BaBar results drastically change the slope of the error ellipses. The differing colors represent the 1-5 σ contours.

References

- [1] Heavy Flavor Averaging Group, Y. Amhis *et al.*, *Averages of b -hadron, c -hadron, and τ -lepton properties as of early 2012*, arXiv:1207.1158, updated results and plots

	All Measurements	No BaBar $K\pi$	No Belle, BaBar $K\pi$	No Belle, BaBar, CDF $K\pi$
x [%]	0.534 ± 0.173	0.533 ± 0.174	0.503 ± 0.174	0.501 ± 0.175
y [%]	0.656 ± 0.093	0.656 ± 0.092	0.649 ± 0.091	0.652 ± 0.090
$\delta_{K\pi}$ [deg]	16.520 ± 9.743	16.264 ± 9.806	14.640 ± 10.356	14.172 ± 10.429
R_D [10^{-3}]	3.579 ± 0.047	3.571 ± 0.047	3.551 ± 0.046	3.551 ± 0.047
$ q/p $ [%]	99.388 ± 1.256	99.403 ± 1.261	99.363 ± 1.327	99.368 ± 1.320
χ^2/ndf	23.9035/26	28.1998/21	28.5592/16	17.723/13

Table 6: Output values of No Direct CPV allowed global fit, excluding the preliminary LHCb A_Γ results from the fit. Different columns list subsets of allowed data.

	All Measurements	No BaBar $K\pi$	No Belle, BaBar $K\pi$	No Belle, BaBar, CDF $K\pi$
x [%]	0.534 ± 0.173	0.533 ± 0.173	0.503 ± 0.174	0.501 ± 0.175
y [%]	0.656 ± 0.093	0.656 ± 0.093	0.649 ± 0.091	0.652 ± 0.091
$\delta_{K\pi}$ [deg]	16.520 ± 9.746	16.269 ± 9.803	14.645 ± 10.352	14.174 ± 10.438
R_D [10^{-3}]	3.579 ± 0.047	3.571 ± 0.047	3.551 ± 0.046	3.551 ± 0.047
$ q/p $ [%]	99.329 ± 1.219	99.344 ± 1.224	99.300 ± 1.288	99.307 ± 1.282
χ^2/ndf	24.2399/28	28.5374/23	28.8959/18	18.0602/15

Table 7: Output values of No Direct CPV allowed global fit, including the preliminary LHCb A_Γ results from the fit. Different columns list subsets of allowed data.

	All Measurements	No BaBar $K\pi$	No Belle, BaBar $K\pi$	No Belle, BaBar, CDF $K\pi$
x [%]	0.534 ± 0.173	0.533 ± 0.174	0.503 ± 0.174	0.501 ± 0.175
y [%]	0.655 ± 0.093	0.656 ± 0.092	0.649 ± 0.091	0.652 ± 0.090
$\delta_{K\pi}$ [deg]	16.506 ± 9.752	16.268 ± 9.805	14.644 ± 10.341	14.170 ± 10.429
R_D [10^{-3}]	3.578 ± 0.047	3.571 ± 0.047	3.551 ± 0.046	3.551 ± 0.047
ϕ [deg]	0.286 ± 0.590	0.2784 ± 0.590	0.284 ± 0.593	0.280 ± 0.587
χ^2/ndf	23.9035/26	28.1998/21	28.5592/16	17.723/13

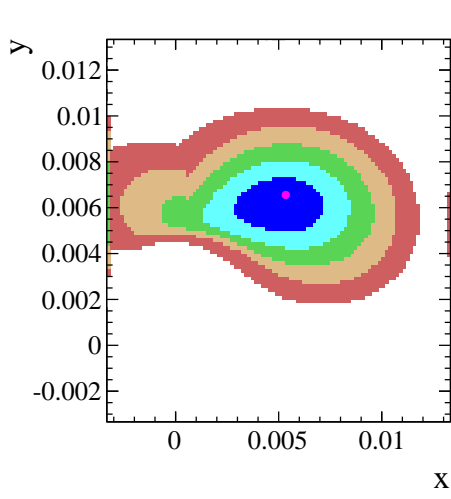
Table 8: Output values of No Direct CPV allowed global fit, with $|q/p|$ fixed. These results exclude the preliminary LHCb A_Γ results from the fit. Different columns list subsets of allowed data.

	All Measurements	No BaBar $K\pi$	No Belle, BaBar $K\pi$	No Belle, BaBar, CDF $K\pi$
x [%]	0.534 ± 0.173	0.533 ± 0.173	0.503 ± 0.174	0.502 ± 0.175
y [%]	0.656 ± 0.093	0.656 ± 0.093	0.649 ± 0.091	0.652 ± 0.091
$\delta_{K\pi}$ [deg]	16.519 ± 9.745	16.268 ± 9.185	14.644 ± 10.340	14.241 ± 10.425
R_D [10^{-3}]	3.579 ± 0.047	3.571 ± 0.047	3.551 ± 0.046	3.551 ± 0.047
ϕ [deg]	0.315 ± 0.573	0.307 ± 0.573	0.312 ± 0.576	0.307 ± 0.569
χ^2/ndf	24.2399/28	28.5374/23	28.8959/18	18.0602/15

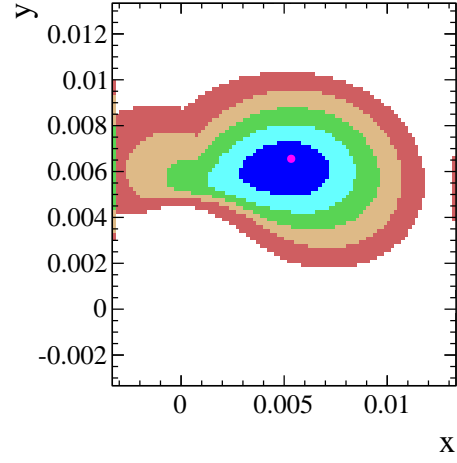
Table 9: Output values of No Direct CPV allowed global fit, fixing $|q/p|$ and fitting for ϕ . These results include the preliminary LHCb A_Γ results in the fit. Different columns list subsets of allowed data.

	All Measurements	No BaBar $K\pi$	No Belle, BaBar $K\pi$	No Belle, BaBar, CDF $K\pi$
x [%]	0.351 ± 0.168	0.472 ± 0.173	0.481 ± 0.177	0.472 ± 0.178
y [%]	0.617 ± 0.074	0.646 ± 0.089	0.650 ± 0.090	0.670 ± 0.091
$\delta_{K\pi}$ [deg]	5.619 ± 13.208	14.155 ± 10.529	14.668 ± 10.500	14.804 ± 10.280
ϕ [deg]	-4.182 ± 7.333	-4.045 ± 6.518	-4.540 ± 6.467	-11.964 ± 10.985
R_D^- [10^{-3}]	3.504 ± 0.048	3.581 ± 0.056	3.595 ± 0.062	3.620 ± 0.073
R_D^+ [10^{-3}]	3.441 ± 0.046	3.501 ± 0.052	3.501 ± 0.056	3.486 ± 0.056
$ q/p $ [%]	98.492 ± 7.100	97.258 ± 8.877	96.831 ± 8.942	88.159 ± 11.870
χ^2/ndf	56.9696/27	32.5589/21	27.9083/15	16.5136/12

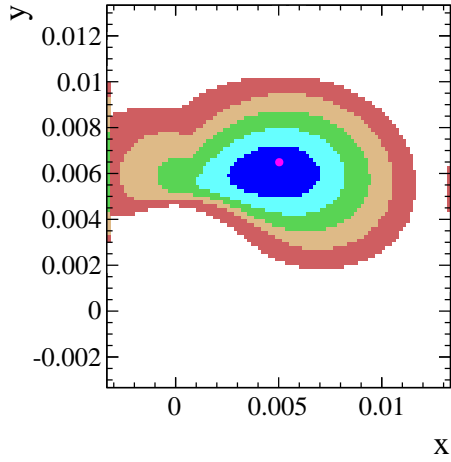
Table 10: Output of the All CP Violation allowed global fit excluding the preliminary LHCb A_Γ measurement. Different Columns list differing subsets of data included in the fit.



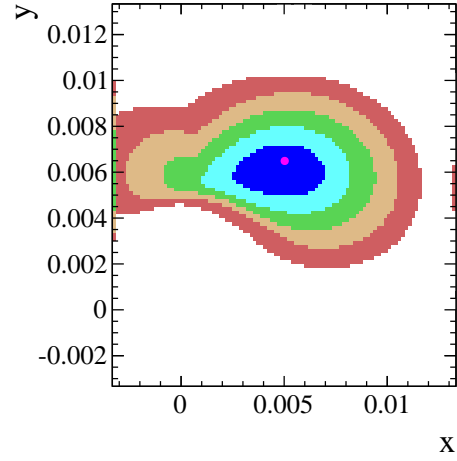
(a) Two dimensional error ellipses for x and y from fit to all listed data.



(b) Two dimensional error ellipses for x and y from fit to all data except LHCb A_Γ .



(c) x vs y for Data excluding Belle and Babar $K\pi$ results.

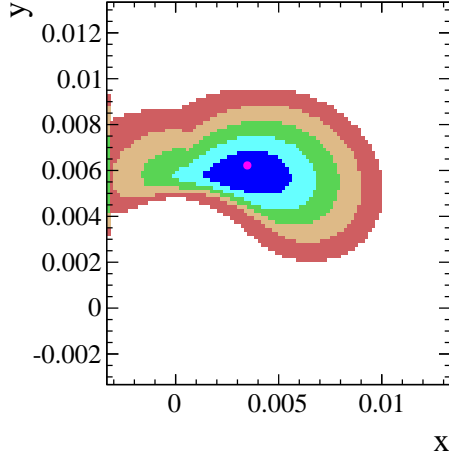


(d) Two dimensional error ellipses for x and y for No Direct CPV, excluding Belle and BaBar $K\pi$ results, and excluding LHCb A_Γ .

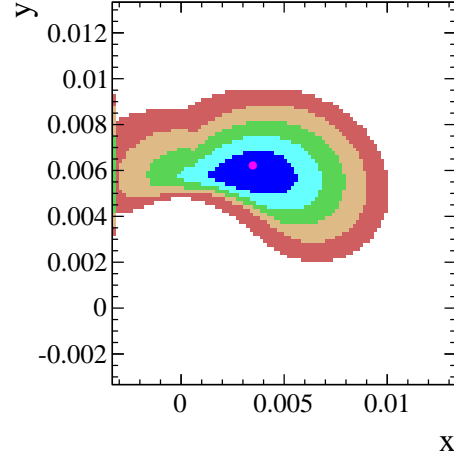
Figure 2: Two dimensional error ellipses of fit for All CPV including differing sets of data for x vs y . The biggest differences come from including the CDF result, which elongates the error ellipses. The differing colors represent the $1-5\sigma$ contours.

	All Measurements	No BaBar $K\pi$	No Belle, BaBar $K\pi$	No Belle, BaBar, CDF $K\pi$
x [%]	0.348 ± 0.168	0.466 ± 0.173	0.475 ± 0.176	0.453 ± 0.175
y [%]	0.622 ± 0.075	0.653 ± 0.089	0.658 ± 0.090	0.688 ± 0.085
$\delta_{K\pi}$ [deg]	6.588 ± 13.002	14.990 ± 10.411	15.655 ± 10.365	16.890 ± 9.103
ϕ [deg]	-3.809 ± 7.379	-4.163 ± 6.577	-4.659 ± 6.541	-12.547 ± 10.953
R_D^- [10^{-3}]	3.500 ± 0.048	3.577 ± 0.057	3.591 ± 0.062	3.621 ± 0.075
R_D^+ [10^{-3}]	3.447 ± 0.044	3.507 ± 0.051	3.508 ± 0.054	3.491 ± 0.054
$ q/p $ [%]	97.994 ± 7.188	96.316 ± 8.725	95.801 ± 8.777	86.862 ± 11.394
χ^2/ndf	57.5868/29	33.157/23	28.5354/17	17.063/14

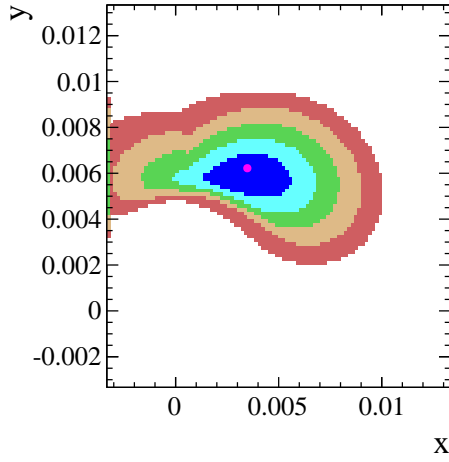
Table 11: Output of the All CP Violation allowed global fit, including the preliminary LHCb A_Γ measurement. Different Columns list differing subsets of data included in the fit.



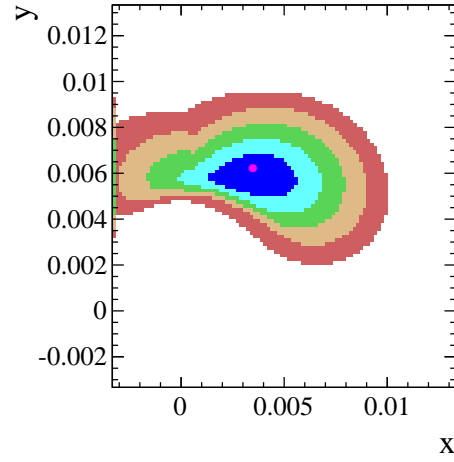
(a) Two dimensional error ellipses for x and y from fit excluding Belle and BaBar $K\pi$ results. Does not include latest A_Γ result of LHCb.



(b) Two dimensional error ellipses for x and y from fit excluding Belle and BaBar $K\pi$ results. Include latest A_Γ result of LHCb.

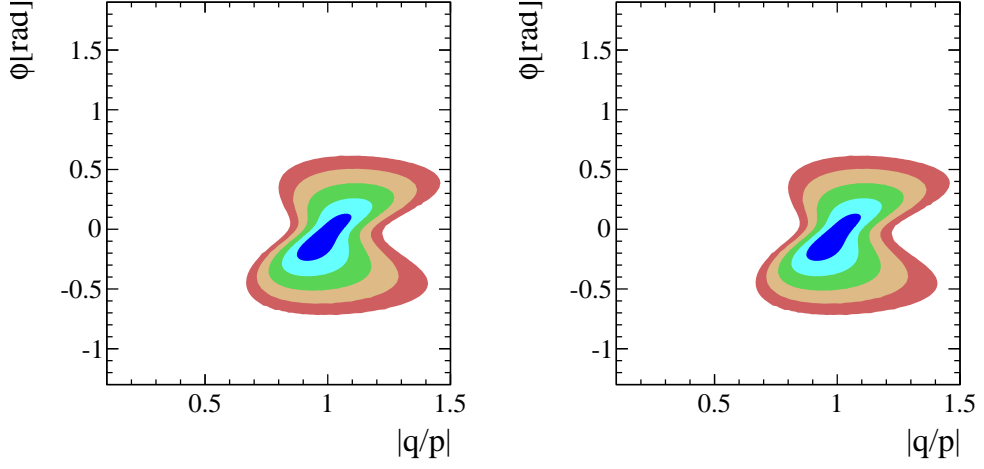


(c) Two dimensional error ellipses for x and y from fit excluding Belle, BaBar and CDF $K\pi$ results. Does not include latest A_Γ result of LHCb.



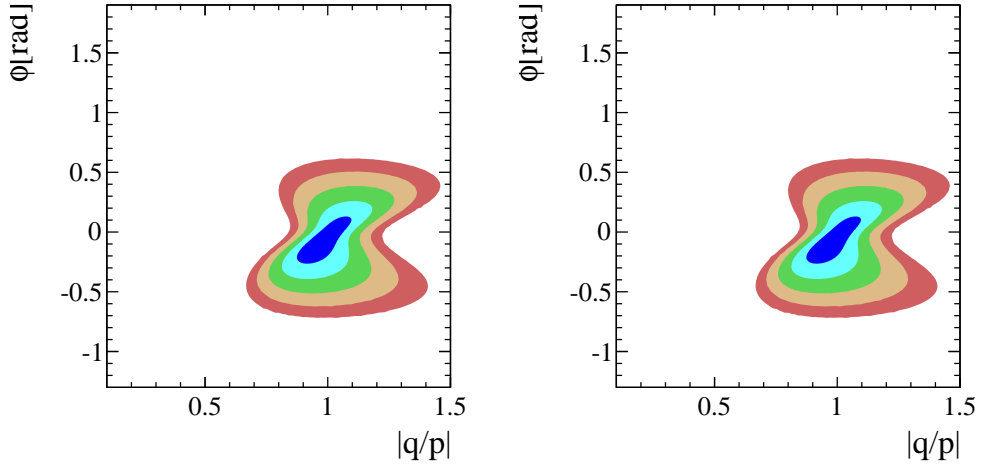
(d) Two dimensional error ellipses for x and y from fit excluding Belle, BaBar and CDF $K\pi$ results. Include latest A_Γ result of LHCb.

Figure 3: Two dimensional error ellipses of fit for All CPV including differing sets of data for x vs y . The biggest differences come from including the CDF result, which elongates the error ellipses. The differing colors represent the 1-5 σ contours.



(a) Two dimensional error ellipses for x and y from fit excluding Belle and BaBar $K\pi$ results. Does not include latest A_Γ result of LHCb.

(b) Two dimensional error ellipses for x and y from fit excluding Belle and BaBar $K\pi$ results. Include latest A_Γ result of LHCb.



(c) Two dimensional error ellipses for x and y from fit excluding Belle, BaBar and CDF $K\pi$ results. Does not include latest A_Γ result of LHCb.

(d) Two dimensional error ellipses for x and y from fit excluding Belle, BaBar and CDF $K\pi$ results. Include latest A_Γ result of LHCb.

Figure 4: Two dimensional error ellipses of fit for All CPV including differing sets of data for ϕ vs q/p . The biggest differences come from including the CDF result, which elongates the error ellipses. The differing colors represent the 1-5 σ contours.